A Haar Wavelet Study on Convective-Radiative Fin under Continuous Motion with Temperature-Dependent Thermal Conductivity

Adivi Sri Venkata RAVI KANTH[1,*] and Niyan UDAY KUMAR[2]

[1]Department of Mathematics, National Institute of Technology, Kurukshetra 136119 (Haryan), India
[2]Division of Fluid Dynamics, School of Advanced Sciences, VIT University, Vellore, Tamil Nadu, India

([*]Corresponding author's e-mail: asvravikanth@yahoo.com)

Abstract

In this paper, the Haar wavelet method is applied to find an approximate solution for heat transfer in moving fins with temperature-dependent thermal conductivity losing heat through both convection and radiation to the surroundings. The effects of various significant parameters involved in the problem, such as the thermal conductivity parameter a, sink temperature θ_a, convection-radiation parameter N_c, radiation-conduction parameter N_r, and Peclet number Pe on the temperature profile of the fin, is discussed and physical interpreted through illustrative graphs.

Keywords: Haar wavelets, extended surface, convective-radiative heat transfer, temperature-dependent thermal conductivity, Newton's method

Introduction

Fins are generally used as a medium for enhancing heat transfer to or from the environment. The amount of heat transfer depends upon the amount of conduction, convection, or radiation of an object. Adding a fin to an object increases the surface area of the object exposed to the surroundings and hence facilitates the rate of heat transfer. Fins are extensively used in various industrial applications, such as heat exchanging devices in car radiators, coolants in refrigerators, and heat exchangers in power plants, etc. An extensive study on an analytical solution to evaluate the temperature distribution of fins is available in [1-3]. The solutions to heat transfer problems are based on the assumption that all the thermo-physical properties, including thermal conductivity and heat transfer coefficients, are constant. However, in practical situations with a high temperature difference between the fin base and its tip, variation of the thermal conductivity of the fin with temperature should be considered. Variable thermal conductivity introduces nonlinearity, which affects the energy balance equation and its solution. Chiu and Chen [4] utilized the Adomian decomposition method to evaluate the efficiency and optimal length of convective rectangular fins with variable thermal conductivity. The Adomian decomposition method was presented by Arslanturk [5] to evaluate the temperature distribution within the fins, and also evaluated the efficiency of the fin. Rajabi [6] studied the efficiency of straight fins with temperature-dependent thermal conductivity using the homotopy perturbation method. A series form analytical solution using the homotopy analysis method was presented for evaluating the fin efficiency of straight convective fins in [7]. Ganji *et al*. [8] used the differential transformation method for studying the effect of temperature dependent thermal conductivity on the fin efficiency of straight convective fins. Kulkarni and Joglekar [9] implemented a numerical technique based on residue minimization to solve the nonlinear differential equation governing the temperature distribution in straight-convective fins having temperature-dependent thermal conductivity, and further evaluated the fin efficiency. In [10] a simplex search method was used to evaluate the temperature field for a conductive-convective fin with variable thermal conductivity. A two-parameter perturbation method was used to evaluate the temperature distribution in conducting-convecting-radiating fins with temperature dependent thermal conductivity in [11]. Nguyen and Aziz [12] studied the performance of different kinds of fins, namely rectangular, trapezoidal, triangular, and

concave parabolic shapes using the finite difference method, and showed the effect of different profile shapes on the heat transfer rate and fin efficiency. Yu and Chen [13] investigated the optimal fin length of convective-radiative rectangular fins with variable thermal conductivity with the help of the Taylor transformation method. In [14] the efficiency of double optimal linearization method was compared with the homotopy perturbation method, variational method and double series regular perturbation method in evaluating the temperature distribution in straight convective-radiative fins with variable thermal conductivity. Recently, moving fins with both convective and radiative heat transfer have been studied by a number of authors viz. Aziz and Khani [15] presented the homotopy analysis method for the analytic solution of heat transfer in moving fins with variable thermal conductivity losing heat to the surroundings simultaneously through convection and radiation. A numerical study of the heat process in continuously moving rods undergoing thermal processing of variable thermal conductivity losing heat by both convection and radiation was studied in [16]. The differential transformation method was applied by Torabi *et al*. [17] for analyzing the heat transfer in moving fins with temperature dependent thermal conductivity, losing heat through both convection and radiation.

In the present paper, the Haar wavelet method is introduced as an alternative approach to study the temperature distribution along convective-radiative fins with temperature-dependent thermal conductivity. With the present method, it is possible to obtain highly accurate results, which is one of the major concerns of applied mathematicians and engineers for solving problems arising in scientific and industrial applications. To verify the accuracy of the present approach, the Haar solutions are compared with the numerical solutions obtained through the standard fourth-order Runge-Kutta method using MATLAB software.

In last few years wavelet based algorithms have become an important and convenient tool in the field of numerical approximations. One of the popular families of wavelets is Haar wavelets, which are wavelets made up of pair of a piecewise constant functions, and are the simplest orthonormal wavelets with compact support. Due to its mathematical simplicity and computationally efficiency, the Haar wavelets have turned out to be an efficient tool for solving initial and boundary value problems. Chen and Hsiao [18] introduced the concept of Haar wavelets as an operational matrix of integration for solving the problems of dynamical systems. The applications of Haar wavelets were used to solve linear and nonlinear stiff systems in [19,20]. Maleknejad [21] suggested a rationalized Haar wavelet approach to solve a system of linear integro-differential equations. Lepik [22] developed a segmentation method based on Haar wavelets for the solution of ODEs and PDEs, and subsequently the method was used to solve nonlinear integro-differential equations in [23]. A Haar wavelet based method to analyze the design in a generalized state space singular system of transistor circuits was presented in [24]. Babolian and Shahsavaran [25] used the Haar wavelet method to obtain the approximate solutions of nonlinear Fredholm integral equations of second kind. Hariharan [26] presented a Haar wavelet based method for solving Fisher's equation. Siraj *et al*. [27] have used uniform Haar wavelets in order to obtain the numerical solutions of 2 point boundary value problems arising in various engineering applications. A spectral collocation method based on Haar wavelets for solving Poisson and biharmonic equations was presented in [28]. Zhi and Yong-yan [29] have devised a computational method based on the use of Haar wavelets for solving higher order eigen value problems. Recently, in [30], the solutions of 2D and 3D Poisson and biharmonic equations were presented by means of Haar wavelets.

Mathematical formulation

Now, the problem description for a continuously moving fin with temperature-dependent thermal conductivity losing heat to the environment through both convection and radiation is presented. A straight convective-radiative fin of cross-sectional area A with perimeter P and moving horizontally with a constant velocity v is considered. The heated fin emerges from a hotter environment at a constant temperature T_b to a colder environment. A common sink temperature $T_a < T_b$ is assumed for both convection and radiation. The thermal conductivity of the material of the fin is assumed to be a linear function of temperature according to;

$$k(T) = k_a[1 + \beta(T - T_a)], \tag{1}$$

where k_a is the thermal conductivity of the material at temperature T_a and β is a measure of thermal conductivity variation with temperature.

The one-dimensional energy balance equation for the moving fin with a constant speed and losing heat simultaneously through convection and radiation can be written as in Aziz and Khani [15];

$$\frac{d}{dx}\left([1 + \beta(T - T_a)]\frac{dT}{dx}\right) - \frac{hP}{k_aA}(T - T_a) - \frac{\varepsilon\sigma P}{k_aA}(T^4 - T_a^4) - \frac{1}{\alpha}v\frac{dT}{dx} = 0, \tag{2}$$

where $\alpha = k_a/\rho c$ is the thermal diffusivity of the material, h is the constant heat transfer coefficient over the entire surface of the moving fin, ε is the constant emissivity from the surface of the fin due to radiation, ρ is the density of material, c is the specific heat and σ is the Stefan-Boltzmann constant. The axial distance x is measured from the point where the fin emerges and comes in contact with the surrounding fluid as shown in **Figure 1**.
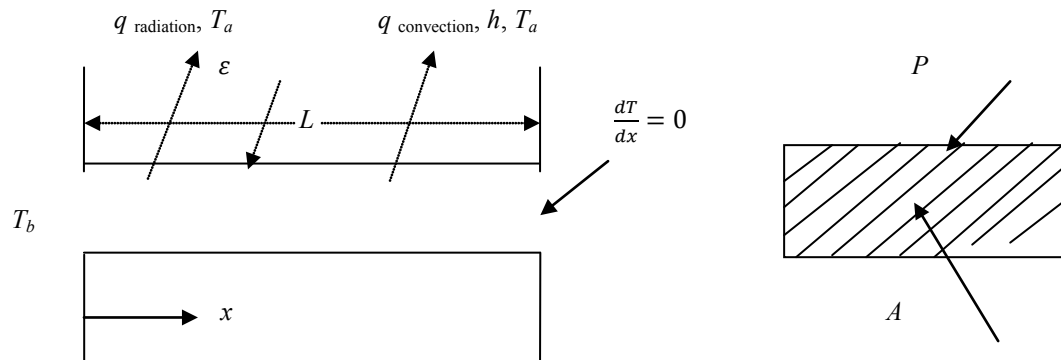

Figure 1 Convection and radiation from the surface of a moving fin.

Making use of the following dimensionless parameters;

$$\theta = \frac{T}{T_b}, \qquad \theta_a = \frac{T_a}{T_b}, \qquad L^* = \frac{PL}{A}, \qquad X = \frac{xL^*}{L}, \tag{3}$$

$$a = \beta T_b, \qquad N_c = \frac{hA}{Pk_a}, \qquad N_r = \frac{\varepsilon\sigma T_b^3 A}{Pk_a}, \qquad Pe = \frac{vA}{P\alpha}, \tag{4}$$

the structure of the Eq. (2) reduces to;

$$\frac{d}{dX}\left([1 + a(\theta - \theta_a)]\frac{d\theta}{dX}\right) - N_c(\theta - \theta_a) - N_r(\theta^4 - \theta_a^4) - Pe\frac{d\theta}{dX} = 0, \tag{5}$$

where L is the length between the point of emergence ($x = 0$) and the point where the temperature gradient in the fin is zero, N_c is the convection-conduction number, N_r is the radiation-conduction number, and Pe is the Peclet number which represents the dimensionless speed of the moving fin. When the material is stationary, $Pe = 0$ and Eq. (5) reduces to that of a stationary fin. For the sake of convenience it is assumed that $L^* = 1$ in the following discussions.

The boundary conditions are given by;

$$X = 0, \qquad \theta(X) = 1, \tag{6}$$

$$X = 1, \qquad \frac{d\theta}{dX}(X) = 0. \tag{7}$$

Haar Wavelets [22]

For the convenience of the readers of this paper, a review of the Haar wavelets is presented. Let $M = 2^J$ (J is the maximal level of resolution); the ith wavelet is defined as;

$$h_i(x) = \begin{cases} 1, & \text{for } x \in [\alpha, \xi), \\ -1, & \text{for } x \in [\xi, \gamma) \quad i = 2, \ldots, 2M \\ 0, & \text{elsewhere} \end{cases} \tag{8}$$

where $\alpha = \frac{k}{2^j}$, $\xi = \frac{k+0.5}{2^j}$, and $\gamma = \frac{k+1}{2^j}$. Here $k = 0, 1, \ldots, 2^j - 1$ is the translation parameter and $j = 0, 1, \ldots, J$ is the dilatation parameter. The number of wavelets is given by $i = 2^j + k + 1$, and the maximum value is $i = 2M$.

For $i = 1$, it is assumed that;

$$h_1(x) = \begin{cases} 1, & for \ x \in [0,1). \\ 0, & \text{elsewhere} \end{cases} \tag{9}$$

The following notations are introduced;

$$p_{i,1}(x) = \int_0^x h_i(x')dx', \tag{10}$$

$$p_{i,v+1}(x) = \int_0^x p_{i,v}(x')dx', \qquad i = 2, 3, \ldots \tag{11}$$

These integrals can be evaluated using Eq. (8) and are given by;

$$p_{i,1}(x) = \begin{cases} x - \alpha & \text{for } x \in [\alpha, \xi), \\ \gamma - x & \text{for } x \in [\xi, \gamma), \\ 0 & \text{elsewhere} \end{cases} \tag{12}$$

$$p_{i,2}(x) = \begin{cases} \frac{1}{2}(x - \alpha)^2 & \text{for } x \in [\alpha, \xi), \\ \frac{1}{2^{2j+2}} - \frac{1}{2}(\gamma - x)^2 & \text{for } x \in [\xi, \gamma) \\ \frac{1}{2^{2j+2}} & \text{for } x \in [\gamma, 1) \ , \\ 0 & \text{elsewhere} \end{cases} \tag{13}$$

Also, it is assumed that;

$$C_{i,1} = \int_0^1 p_{i,1}(x')dx'. \tag{14}$$

The collocation points are defined as;

$$X_j = \frac{j - 0.5}{2M}, \qquad j = 1, 2, \ldots, 2M \tag{15}$$

Re-writing Eq. (5) as;

$$\frac{d^2\theta}{dX^2} = f\left(X, \theta, \frac{d\theta}{dX}\right). \tag{16}$$

The Haar wavelet method for the above nonlinear problem subject to the boundary conditions is now discussed;

$$\theta(0) = \lambda_1, \quad \theta'(1) = \lambda_2. \tag{17}$$

Following Chen and Hsiao [18], it is assumed that;

$$\theta''(X) = \sum_{i=1}^{2M} a_i h_i(X). \tag{18}$$

Integrating Eq. (18) from 0 to X, the derivative $\theta'(X)$ can be expressed as;

$$\theta'(X) = \theta'(0) + \sum_{i=1}^{2M} a_i p_{i,1}(X). \tag{19}$$

Putting $X = 1$ in Eq. (19) and using the second boundary condition, the value of $\theta'(0) = \lambda_2 - a_1$ is obtained.

Now, Eq. (19) can be written as;

$$\theta'(X) = (\lambda_2 - a_1) + \sum_{i=1}^{2M} a_i p_{i,1}(X). \tag{20}$$

Now, again integrating Eq. (20) from 0 to X and using the first boundary condition;

$$\theta(X) = \lambda_1 + (\lambda_2 - a_1)X + \sum_{i=1}^{2M} a_i p_{i,2}(X) \tag{21}$$

is obtained. Substituting the values of $\theta(X)$, $\theta'(X)$ and $\theta''(X)$ in Eq. (16) and applying discretization using collocation points given in Eq. (15), a nonlinear system is obtained;

$$\sum_{i=1}^{2M} a_i h_i(X_j) = \left[f\left(X_j, \lambda_1 + (\lambda_2 - a_1)X_j + \sum_{i=1}^{2M} a_i p_{i,2}(X_j)\right), (\lambda_2 - a_1) + \sum_{i=1}^{2M} a_i p_{i,1}(X_j)\right] \tag{22}$$

Solving the above $2M \times 2M$ system using Newton's method the unknown Haar coefficients $a_i's$, $i = 1, 2,\ldots, 2M$ are obtained, which are eventually used to find the approximate solution.

Theorem: Let $f(x) \in L^2(R)$ be a continuous function defined on $(0, 1)$. Then, the error norm at J^{th} level satisfies the following inequality;

$$\|E_j\| \le \frac{K^2}{12} 2^{-2J},$$

where $|f'(x)| \le K$, $\forall x \in (0,1)$ and $K > 0$ and M is a positive number related to the Jth level resolution of the wavelet given by $M = 2^J$.

Proof. See ref. [25]. It is observed that the error norm at J^{th} level is inversely proportional to the level of resolution of the Haar wavelet, which ensures convergence of the method.

Results and discussion

In this section numerical results for temperature distribution in the fin, fin-tip temperature and fin-base heat transfer for various values of significant parameters involved in the problem are provided. Also, the behavior of parameters and its effect on the temperature distribution, heat transfer characteristics has been studied. In particular, the effect of thermal conductivity parameter (a), sink temperature (θ_a), convection-conduction parameter (N_c), radiation-conduction parameter (N_r), and Peclet number (Pe) are examined and are shown graphically in **Figures 2 - 6**.

Table 1 presents the comparison of temperature distribution in the fin for $a = 0.6$, $\theta_a = 0.2$, $N_c = 4$, $N_r = 4$ and $Pe = 3$. It can be clearly seen that the Haar solution (HS) matches with the numerical solution (NS). Moreover, the accuracy of the solution can be increased by increasing the level of resolution of the wavelets.

Table 1 Temperature distribution in the fin for $a = 0.6$, $\theta_a = 0.2$, $N_c = 4$, $N_r = 4$ and $Pe = 3$.

X	$\theta(X)$	
	HS	NS
0.0	1	1
0.1	0.902371	0.902372
0.2	0.821278	0.821279
0.3	0.752982	0.752984
0.4	0.695052	0.695055
0.5	0.645945	0.645947
0.6	0.604781	0.604783
0.7	0.571260	0.571262
0.8	0.545663	0.545664
0.9	0.528930	0.528928
1.0	0.522806	0.522800

The tables for fin-tip temperature and fin-base heat transfer are so constructed that the individual effect of each parameter on the temperature and heat characteristics can be clearly seen in the absence of other parameters. The comparison of fin-tip temperature (1) for a stationary fin (i.e. $Pe = 0$) is provided in **Table 2a** for different values of a, θ_a, N_c, N_r. In **Table 2b** the same data of fin-tip temperature is provided, but for the case of a moving fin (i.e. $Pe = 3$).

Table 2a Comparison of fin-tip temperature for a stationary fin ($Pe = 0$).

θ_a	a	N_c	N_r	$\theta(1)$	
				HS	NS
0	0	0	0	1	1
	0	0	1	0.779145	0.779148
	0	2	0	0.459098	0.459098
	0	2	1	0.435646	0.435694
	0.6	0	0	1	1
	0.6	0	1	0.826746	0.826747
	0.6	2	0	0.566285	0.566280
	0.6	2	1	0.531579	0.531575
0.8	0	0	0	1	1
	0	0	1	0.879763	0.879766
	0	2	0	0.891820	0.891820
	0	2	1	0.848914	0.848917
	0.6	0	0	1	1
	0.6	0	1	0.883882	0.883888
	0.6	2	0	0.896590	0.896591
	0.6	2	1	0.852071	0.852073

Table 2b Comparison of fin-tip temperature for a moving fin ($Pe = 3$).

θ_a	a	N_c	N_r	$\theta(1)$ HS	$\theta(1)$ NS
0	0	0	0	1	1
	0	0	1	0.854452	0.854452
	0	2	0	0.658564	0.658560
	0	2	1	0.612390	0.612391
	0.6	0	0	1	1
	0.6	0	1	0.875709	0.875710
	0.6	2	0	0.708550	0.708548
	0.6	2	1	0.661585	0.661583
0.8	0	0	0	1	1
	0	0	1	0.916623	0.916624
	0	2	0	0.931713	0.931713
	0	2	1	0.884040	0.884043
	0.6	0	0	1	1
	0.6	0	1	0.918933	0.918932
	0.6	2	0	0.933931	0.933927
	0.6	2	1	0.886516	0.886515

The amount of the energy transferred from the fin base (i.e., $\theta'(0)$) is of major interest in engineering applications. **Table 3a** is tabulated for comparing the temperature gradient at the fin-base of a stationary fin (i.e. $Pe = 0$) for various values of a, θ_a, N_c, N_r. Further, the same data for a moving fin (i.e. $Pe = 3$) case is provided in **Table 3b**.

Table 3a Comparison of temperature gradient at the fin-base for a stationary fin ($Pe = 0$).

θ_a	a	N_c	N_r	$\theta'(0)$ HS	$\theta'(0)$ NS
0	0	0	0	0	0
	0	0	1	-0.533989	-0.533986
	0	2	0	-1.256366	-1.256367
	0	2	1	-1.419205	-1.419141
	0.6	0	0	0	0
	0.6	0	1	-0.386105	-0.386104
	0.6	2	0	-0.886832	-0.886849
	0.6	2	1	-1.025683	-1.025685
0.8	0	0	0	0	0
	0	0	1	-0.301153	-0.301149
	0	2	0	-0.251273	-0.251273
	0	2	1	-0.418442	-0.418439
	0.6	0	0	0	0
	0.6	0	1	-0.278361	-0.278358
	0.6	2	0	-0.231145	-0.231142
	0.6	2	1	-0.387706	-0.387706

Table 3b Comparison of temperature gradient at the fin-base for a moving fin ($Pe = 3$).

θ_a	a	N_c	N_r	$\theta'(0)$	
				HS	NS
0	0	0	0	0	0
	0	0	1	-0.253258	-0.253258
	0	2	0	-0.551052	-0.551030
	0	2	1	-0.712695	-0.712696
	0.6	0	0	0	0
	0.6	0	1	-0.220383	-0.220383
	0.6	2	0	-0.475111	-0.475115
	0.6	2	1	-0.606611	-0.606609
0.8	0	0	0	0	0
	0	0	1	-0.148200	-0.148199
	0	2	0	-0.110210	-0.110211
	0	2	1	-0.228720	-0.228719
	0.6	0	0	0	0
	0.6	0	1	-0.142904	-0.142903
	0.6	2	0	-0.106692	-0.106697
	0.6	2	1	-0.219308	-0.219307

The influence of the thermal conductivity parameter a on the temperature distribution along the fin for $\theta_a = 0.2$, $N_c = 4$, $N_r = 4$ and $Pe = 3$ is presented in **Figure 2a**. It is clear from the figure that as the thermal conductivity parameter is increased, the temperature distribution along the fin increases. Physically speaking, the effect of increase in thermal conductivity parameter enhances the heat conduction process, and results in an increase in the local temperature of the fin. It is further observed that the fin-tip temperature increases with an increase in thermal conductivity parameter.
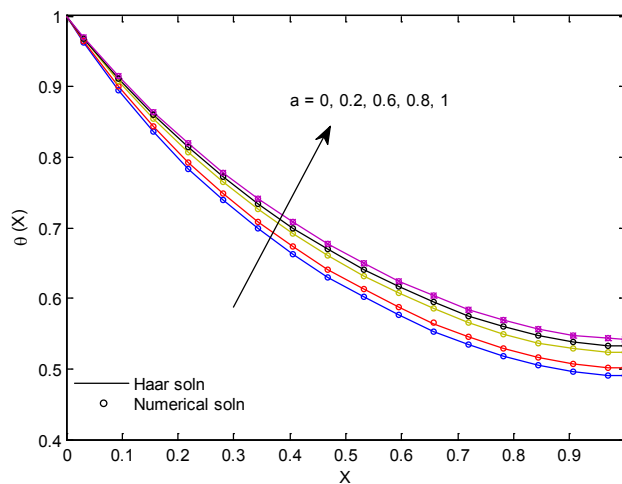
Figure 2a Temperature distribution along a fin for different values of a, with $\theta_a = 0.2, N_c = 4, N_r = 4$ and $Pe = 3$.

In **Figure 2b** the temperature gradient along the fin for different values of a, with $\theta_a = 0.2, N_c = 4, N_r = 4$ and $Pe = 3$ has been plotted. It is observed from the figure that the heat transfer is more prominent for lower values of thermal conductivity parameter. The negative values of the derivative indicate the cooling process of the fin due to heat loss to the surroundings.
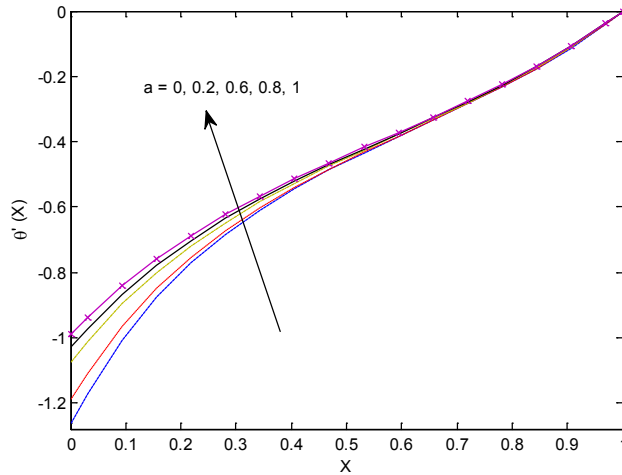

Figure 2b Temperature gradient along the fin for different values of a, with $\theta_a = 0.2, N_c = 4, N_r = 4$ and $Pe = 3$.

Figure 3a depicts the effect of sink temperature θ_a on the temperature profile of the fin for $a = 0.2$, $N_c = 1, N_r = 2$ and $Pe = 3$. From the figure it is observed that temperature distribution in the fin increases with increasing values of the sink temperature. The role of this effect can be understood due to increased conduction in the fin.
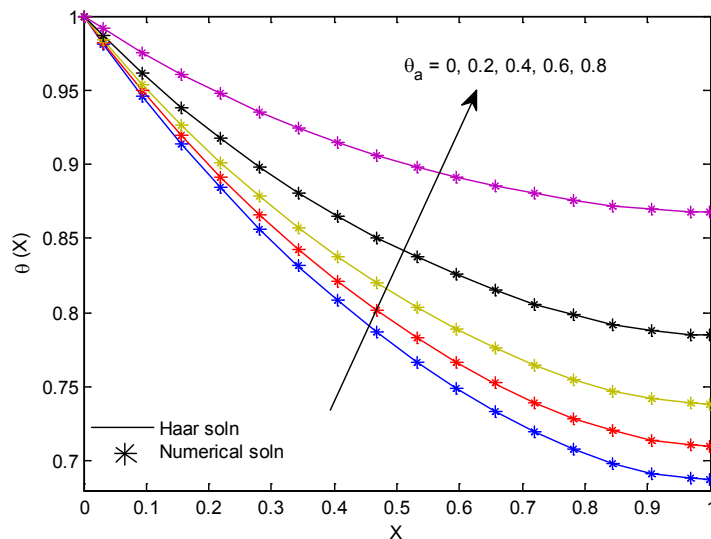
Figure 3a Temperature distribution along the fin for different values of θ_a, with $a = 0.2, N_c = 1, N_r = 2$ and $Pe = 3$.

The graph of temperature gradient in the fin for different values of θ_a, with $a = 0.2$, $N_c = 1$, $N_r = 2$ and $Pe = 3$ has been plotted in **Figure 3b**. It is apparent from the figure that the heat transfer is higher at lower values of the sink temperature. The cause for this effect can be due to the augmented convection and radiation process which results in more heat loss.
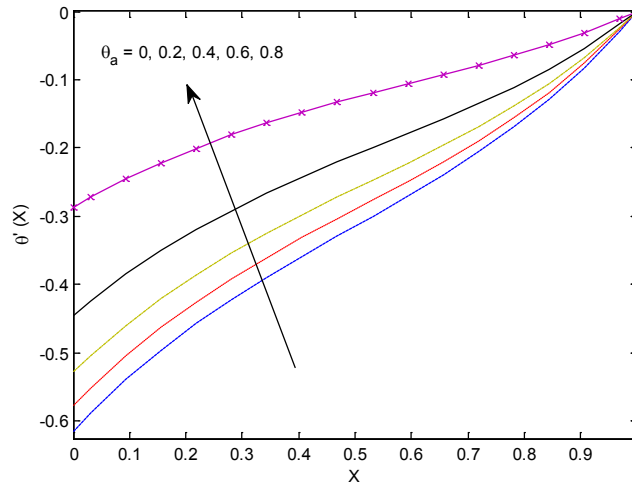

Figure 3b Temperature gradient along the fin for different values of θ_a, with $a = 0.2, N_c = 1, N_r = 2$ and $Pe = 3$.

The effect of convection-conduction parameter N_c on the temperature distribution for $a = 1$, $\theta_a = 0.8, N_r = 0.25$ and $Pe = 2$ is described in **Figure 4a**. It is evident that as the convection-conduction parameter is increased, it attributes to more heat loss from the fin, and hence cooling of the fin occurs, which shows a decrease in the temperature profile. The graph of temperature gradient for $a = 1, \theta_a = 0.8, N_r = 0.25$ and $Pe = 2$ is plotted in **Figure 4b**. It is noticed from the figure that the heat transfer increases with an increase in convection-conduction parameter.
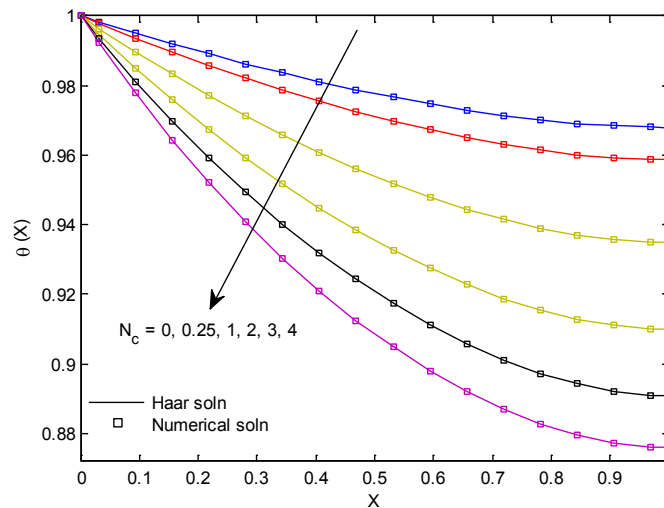

Figure 4a Temperature distribution along the fin for different values of N_c, with $a = 1, \theta_a = 0.8, N_r = 0.25$ and $Pe = 2$.
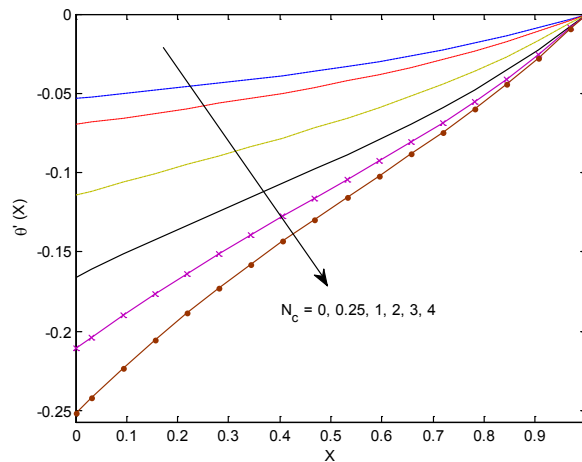
Figure 4b Temperature gradient along the fin for different values of N_c, with $a = 1, \theta_a = 0.8, N_r = 0.25$ and $Pe = 2$.

The variation of temperature distribution for different values of radiation-conduction parameter N_r with $a = 0.6$, $\theta_a = 0.4$, $N_c = 1$ and $Pe = 2.5$ is illustrated in **Figure 5a**. As anticipated, the increase of radiation-conduction parameter amplifies the heat loss rate, which in turn lowers the temperature distribution. **Figure 5b** depicts the temperature gradient for $a = 0.6$, $\theta_a = 0.4$, $N_c = 1$ and $Pe = 2.5$ for different values of the radiation-conduction parameter. Clearly, the figure demonstrates that the heat transfer increases with increasing radiation-conduction parameter. The heat loss due to radiation will be more prevalent if the forced convection is weak or absent or when only natural convection occurs.
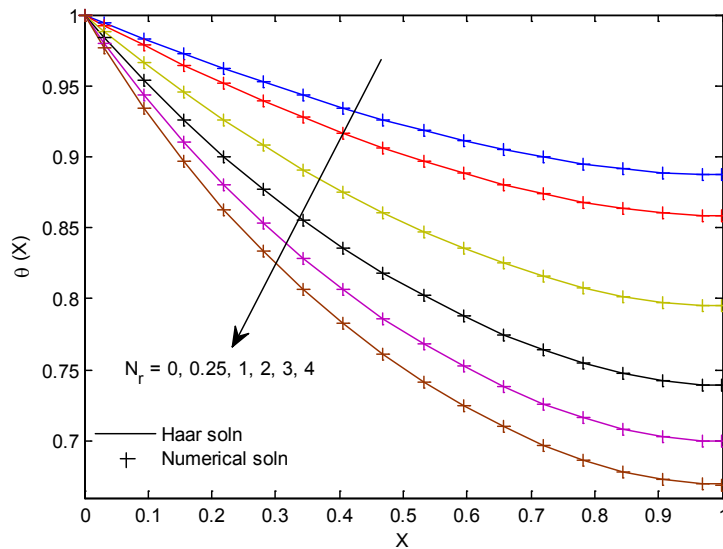

Figure 5a Temperature distribution along the fin for different values of N_r, with $a = 0.6, \theta_a = 0.4, N_c = 1$ and $Pe = 2.5$.
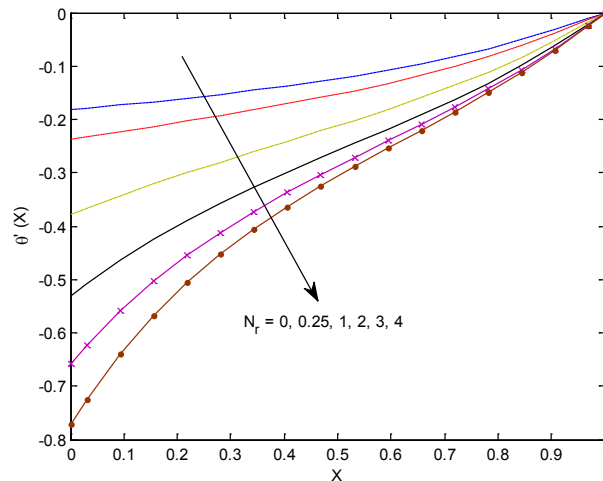
Figure 5b Temperature gradient along the fin for different values of N_r, with $a = 0.6, \theta_a = 0.4, N_c = 1$ and $Pe = 2.5$.

The effect of a dimensionless speed parameter (i.e. the Peclet number) on the temperature profile is elucidated for $a = 0.8$, $\theta_a = 0.6$, $N_c = 0.25$ and $N_r = 1$ in **Figure 6a**. It is evident that the temperature distribution increases with an increase in the Peclet number. This is because as the fin moves more rapidly the exposure time to the surroundings reduces, which results in higher temperature variation. **Figure 6b** is plotted to show the effect of Pe on the heat transfer rate for fixed $a = 0.8$, $\theta_a = 0.6$, $N_c = 0.25$ and $N_r = 1$. Similar results are noticed from the figure that the heat transfer increases as the Peclet number increases.
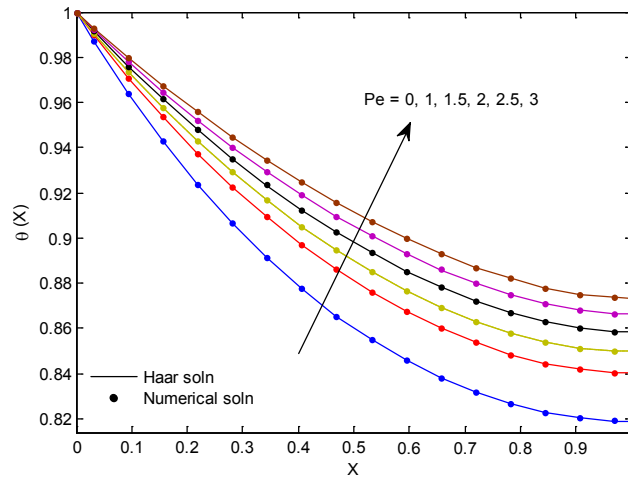

Figure 6a Temperature distribution along the fin for different values of Pe, with $a = 0.8, \theta_a = 0.6, N_c = 0.25$ and $N_r = 1$.
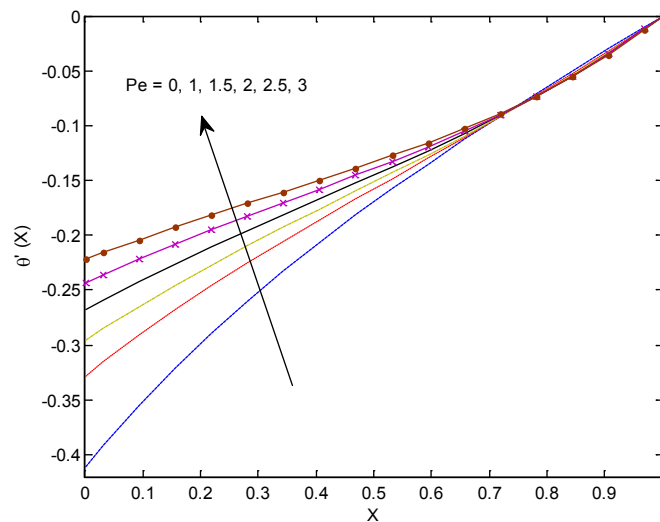
Figure 6b Temperature gradient along the fin for different values of *Pe*, with $a = 0.8, \theta_a = 0.6, N_c = 0.25$ and $N_r = 1$.

Conclusions

In this paper, the effects of the significant parameters i.e. the thermal conductivity parameter (*a*), sink temperature (θ_a), convection-conduction parameter (N_c), radiation-conduction parameter (N_r), Peclet number (*Pe*) on the temperature distribution and heat transfer characteristics of continuously moving convective-radiative fin with temperature-dependent thermal conductivity have been studied. The governing equations are expressed in non-dimensional form and are solved using Haar wavelets. The effects of the relevant parameters on the temperature distribution and heat transfer characteristics have been investigated both numerically and graphically. The Haar wavelet method provides highly accurate and stable results. Also, the method is computationally efficient and the algorithm can be easily implemented on the computer. This ensures that the Haar wavelet method can be used as an alternative tool for solving varied kinds of linear and nonlinear problems arising in science and engineering.

Acknowledgement

References

[1]   DQ Kern and AD Kraus. *Extended Surface Heat Transfer*. McGraw-Hill, New York, 1972.
[2]   AD Kraus, A Aziz and J Welty. *Extended Surface Heat Transfer*. John Wiley and Sons, New York, 2001.
[3]   JH Lienhard IV and JH Lienhard V. *A Heat Transfer Textbook*. Phlogiston Press, Cambridge, Massachusetts, 2003.
[4]   CH Chiu and CK Chen. A decomposition method for solving the convective longitudinal fins with variable thermal conductivity. *Int. J. Heat Mass Tran.* 2002; **45**, 2067-75.
[5]   C Arslanturk. A decomposition method for fin efficiency of convective straight fins with temperature-dependent thermal conductivity. *Int. Commun. Heat Mass Tran.* 2005; **32**, 831-41.
[6]   A Rajabi. Homotopy perturbation method for fin efficiency of convective straight fins with temperature-dependent thermal conductivity. *Phys. Lett. A* 2007; **364**, 33-7.

[7]   G Domairry and M Fazeli. Homotopy analysis method to determine the fin efficiency of convective straight fins with temperature-dependent thermal conductivity. *Commun. Nonlinear Sci. Numer. Simulat*. 2009; **14**, 489-99.

[8]   AA Joneidi, DD Ganji and M Babelahi. Differential transformation method to determine fin efficiency of convective straight fins with temperature dependent thermal conductivity. *Int. Commun. Heat Mass Tran*. 2009; **36**, 757-62.

[9]   DB Kulkarni and MM Joglekar. Residue minimization technique to analyze the efficiency of convective straight fins having temperature-dependent thermal conductivity. *Appl. Math. Comput*. 2009; **215**, 2184-91.

[10] R Das. A simplex search method for a conductive-convective fin with variable conductivity. *Int. J. Heat Mass Tran*. 2011; **54**, 5001-9.

[11] A Aziz and JY Benzies Application of perturbation techniques to heat-transfer problems with variable thermal properties. *Int. J. Heat Mass Tran*. 1976; **19**, 271-6.

[12] H Nguyen and A Aziz. Heat transfer from convecting-radiating fins of different profile shapes. *Warme und Stoffubertragung* 1992; **27**, 67-72.

[13] LT Yu and CK Chen. Application of Taylor transformation to optimize rectangular fins with variable thermal parameters. *Appl. Math. Model*. 1998; **22**, 11-21.

[14] MN Bouaziz and A Aziz. Simple and accurate solution for convective-radiative fin with temperature dependent thermal conductivity using double optimal linearization. *Energ. Convers. Manage*. 2010; **51**, 2276-782.

[15] A Aziz and F Khani. Convection-radiation from a continuous moving fin of variable thermal conductivity. *J. Franklin Inst*. 2011; **348**, 640-51.

[16] A Aziz and RJ Lopez. Convection-radiation from a continuously moving, variable thermal conductivity sheet or rod undergoing thermal processing. *Int. J. Therm. Sci*. 2011; **50**, 1523-31.

[17] M Torabi, H Yaghoobi and A Aziz. Analytical solution for convective-radiative continuously moving fin with temperature-dependent thermal conductivity. *Int. J. Thermophys*. 2012; **33**, 924-41.

[18] CF Chen and CH Hsiao. Haar wavelet method for solving lumped and distributed-parameter systems. *IEEE Proc. Control Theory Appl*. 1997; **144**, 87-94.

[19] CH Hsiao and WJ Wang. Haar wavelet approach to nonlinear stiff systems. *Math. Comput. Simulat*. 2001; **57**, 347-53.

[20] CH Hsiao. Haar wavelet approach to linear stiff systems. *Math. Comput. Simulat*. 2004; **64**, 561-7.

[21] K Maleknejad, F Mirzaee and S Abbasbandy. Solving linear integro-differential equations system by using rationalized Haar functions method. *Appl. Math. Comput*. 2004; **155**, 317-28.

[22] U Lepik. Numerical solution of differential equations using Haar wavelets. *Math. Comput. Simulat*. 2005; **68**, 127-43.

[23] U Lepik. Haar wavelet method for nonlinear integro-differential equations. *Appl. Math. Comput*. 2006; **176**, 324-33.

[24] R Kalpana and SR Balachandar. Haar wavelet method for the analysis of transistor circuits. *Int. J. Electron. Commun*. 2007; **61**, 589-94.

[25] E Babolian and A Shahsavaran. Numerical solution of nonlinear Fredholm integral equations of the second kind using Haar wavelets. *J. Comput. Appl. Math*. 2009; **225**, 87-95.

[26] G Hariharan, K Kannan and KR Sharma. Haar wavelet method for solving Fisher's equation. *Appl. Math. Comput*. 2009; **211**, 284-92.

[27] S Ul-Islam, I Aziz and B Sarler. The numerical solution of second-order boundary-value problems by collocation method with the Haar wavelets. *Math. Comput. Model*. 2010; **52**, 1577-90.

[28] S Zhi and C Yong-yan. A spectral collocation method based on Haar wavelets for Poisson equations and biharmonic equations. *Math. Comput. Model*. 2011; **54**, 2858-68.

[29] S Zhi and C Yong-yan. Application of Haar wavelet method to eigen value problems of high order differential equations. *Appl. Math. Model*. 2012; **36**, 4020-6.

[30] S Zhi and C Yong-yan. Solving 2D and 3D Poisson equations and biharmonic equations by the Haar wavelet method. *Appl. Math. Model*. 2012; **36**, 5143-61.